Poster 226
AMS January 2019 Meeting
Extended Abstract

226. Preliminary Case Study of Geostationary IR Sounding Data from FY-4A GIIRS

Jessica Gartzke
Robert Knuteson, William L. Smith, Elisabeth Weisz, Hank Revercomb & Paul Menzel
Univ. of Wisconsin-Madison Space Science and Engineering Center

1. Introduction

1.1 Abstract

A hyperspectral Infrared sounder, the Geostationary Interferometric Infrared Sounder (GIIRS), is operational aboard the Chinese Fengyun-4A satellite. The GIIRS has a spectral resolution in the thermal infrared which matches the JPSS CrIS sensors on S-NPP and NOAA-20. It is the first geostationary interferometer that provides continuous soundings of temperature and humidity which has been successfully launched into Earth orbit. A series of GIIRS sensors will obtain roughly hourly vertical profiles of the atmosphere, which is invaluable for near real-time tracking of the pre-convective storm environment. The first GIIRS has more limited spatial coverage than the subsequent sensors. Retrieved profiles have been processed by the China Meteorological Administration (CMA) and are publicly available. In this study, comparisons are made between CMA GIIRS-derived vertical profiles of temperature and humidity and local observational data from coincident radiosonde launch sites, e.g. at Shanghai, China and Darwin, Australia. This activity is part of an assessment being performed at SSEC/CIMSS of the characteristics of the GIIRS radiances and the suitability of assimilation into NWP models. This paper is a preliminary study into the new GIIRS data from CMA.

1.2 Data

Three different data types were used in this preliminary study including FY4A GIIRS, WMO radiosonde network and the MADIS surface station network. Each data provides different temporal, spatial and measurement resolutions. By utilizing all three of these data, comparisons can be made between them.

1.2.1 GIIRS Infrared Sounder

Satellite data from Fengyun-4A (FY-4A) GIIRS was used for analysis in this study. The FY-4A satellite is in geostationary orbit and is operated by the China Meteorological Administration (Yang, Zhang, Wei, Lu, & Guo, 2017). Launched on 10 December 2016, it was re-located from the initial position (99.5°E) to the current operational position (105°E nominal) on 16 April 2018. Four instruments fly on FY-4A including the Lightning Mapping Imager (LMI), the Advanced Geostationary Radiation Imager (AGRI), the Space Environment Package (SEP) and the Geostationary Interferometric Infrared Sounder (GIIRS).

The GIIRS data was obtained from http://satellite.nsmc.org.cn using the file names FY4A-_GIIRS-_N_REGC_1047E_L2-_AVP-.nc and FY4A-_GIIRS-_N_DISK_1047E_L2-_AVP.nc. The regional file contains hourly data for the China region. The disk file contains data collected every three hours within the FY4A coverage area. A number of observations are available within each file including atmospheric temperature, atmospheric humidity, surface temperature, pressure, surface pressure, various convective indices, ozone, latitude and longitude. GIIRS uses 101 levels to define the atmosphere. These levels are the same as the fixed AIRS L2 pressure levels. Since FY-4A is in a geostationary orbit over the equator it always has the same field of view. The GIIRS field of regard is indicated in Figure 1 but the soundings are limited to about 60S to 60N.

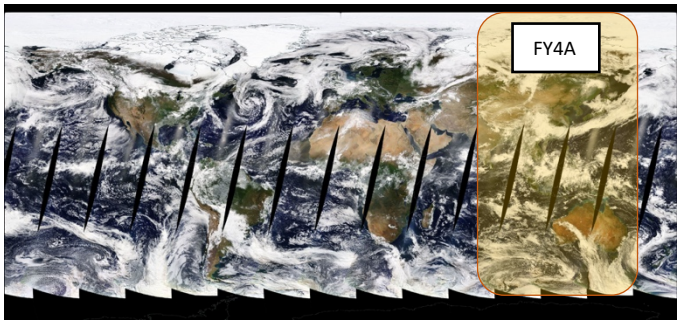

Figure 1. GIIRS domain in the eastern hemisphere.

1.2.2 WMO Radiosonde Network

The World Meteorological Organization (WMO) provides a database with access to about 1300 high quality upper air stations scattered throughout the globe. These data sets are generally made two times a day at 0000 and 1200 UTC, however some countries have slightly different release times and may only make observations once per day. These instruments record pressure, temperature, humidity, wind speed and wind direction throughout the troposphere and stratosphere to about 30 km above the ground. They are run by individual countries meteorological services and the data is collected and made available through the Observing Systems Capability Analysis and Review Tool (OSCAR) https://oscar.wmo.int/surface//index.html#/.

The CMA provides OSCAR with a network of radiosondes known as the CMA radiosonde network. This network currently uses the GTS1 digital radiosonde (Product ID：HQQTdaqi001) (Feng, 2006). Detailed information can be found at https://www.instrumentstrade.com/gts1-digital-radiosonde_p2824.html and reproduced in Table 1.

Bian et al. compared Vaisala RS80, Cryogenic Frostpoint Hygrometer (CFH) and GTS1 radiosondes and found that they have comparable biases (Bian et al., 2011). The average relative dry bias produced by the GFS1 sensor is 10% below 500 hPa, 30% above 500 hPa, and 55% above 310 hPa. For humidity, the GTS1 radiosonde does not respond to humidity changes in the upper troposphere, and sometimes even in the middle troposphere which could cause a humidity bias. The daytime temperature bias is relatively consistent between the Vaisala RS80 and GTS1 but produces biases at night on the order of −0.2 K to −1.6 K (Bian et al., 2011).

In contrast to the CMA's GTS1 network of radiosondes, Australia's Bureau of Meteorology (BOM) currently operates a network of 50 upper air stations. BOM currently uses Vaisala RS92 in their Upper air network and includes most of the data in the OSCAR network (Kottayil et al., 2012). The details of these instruments are shown in Table 2.The RS92 has shown consistent temperature profiles within 0.2 degrees Celsius (Vömel, David, & Smith, 2007). Moisture has been shown to have a dry bias, about 9% at the surface and 50% at 15 km

(Vomel et al., 2007). More information about the RS92 can be found at https://www.vaisala.com/sites/default/files/documents/RS92SGP-Datasheet-B210358EN-F-LOW.pdf

1.2.3 MADIS Surface Stations

Surface station data was used in this study for its high temporal resolution. The NOAA Meteorological Assimilation Data Ingest system (MADIS) provides hourly latitude, longitude, elevation surface temperature, surface dewpoint, surface pressure for a high density of stations in the CONUS and more limited station data throughout the world. This system accumulates data in real time from participating countries, including China. There are about 40 MADIS surface locations throughout the GIIRS domain that can be used for validation. The MADIS Surface locations available within China are shown in Figure 2 and for Australia in Figure 3. Hourly surface observations files in netcdf format were obtained from https://madis-data.ncep.noaa.gov/public/sfcdump.html.

2. Methodology

2.1 Case Study: Shanghai, China

The city of Shanghai in China was chosen for the case study location in this study because of its coastal location and its availability of data. MADIS surface station and radiosonde, GIIRS and local radiosonde data is readily available within a 150 km range. The locations of each data source are shown in Figure 2. Since CMA GIIRS L2 data became operationally available starting May 24, 2018, this case study concentrates on the few weeks following the start date (June 1 to July 15). A number of cases were extracted during this time based on the availability of good data. These days were selected by considering the regional MODIS true color images to determine the local cloud conditions for each day.

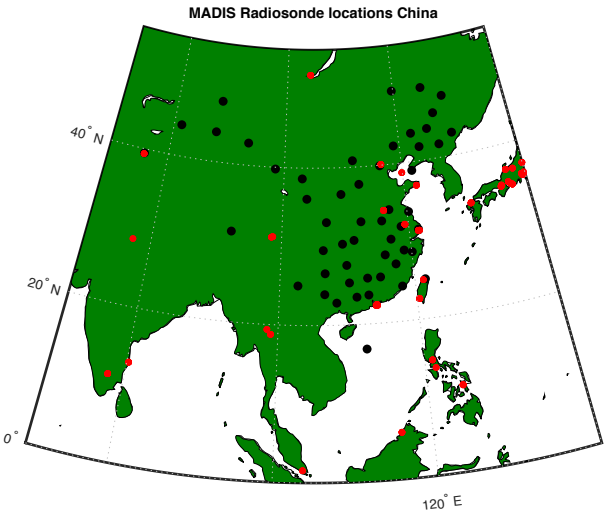

Figure 2 The MADIS (red) and radiosonde (black) locations within China.

2.2 Case Study: Darwin, Australia

The city of Darwin, Australia was chosen for a secondary case study due to its location in the southern hemisphere within the GIIRS domain. Australia has 27 MADIS locations currently operational throughout the country. Darwin's WMO identifier is 94120 and produces soundings at 0 and 12z. In addition, the GIIRS field of view stretches from 15 S to 45 S, fully encompassing the country. The same "clear" days were chosen for both Shanghai and Darwin case studies including June 1 2018, June 11 2018, July 10 2018, July 14 2018 and July 15 2018. Figure 3 shows the MADIS and radiosonde locations within Australia.

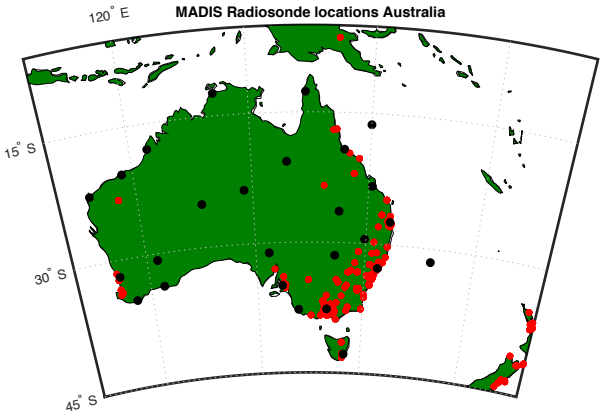

Figure 3 MADIS (red) and radiosonde (black) locations within Australia.

2.3 Gridding GIIRS Data

In order to simplify comparisons between satellite and model data, GIIRS data was converted to a contiguous grid covering the GIIRS domains. The data was gridded onto a roughly 0.7 by 0.7 degree grid which is the same as the ERA-Interim reanalysis grid cells. Data within each grid box is averaged in the horizontal for each retrieval level. Comparisons with NWP models are not included here but are in process of completion. An example of the gridding process is shown in Figure 4.

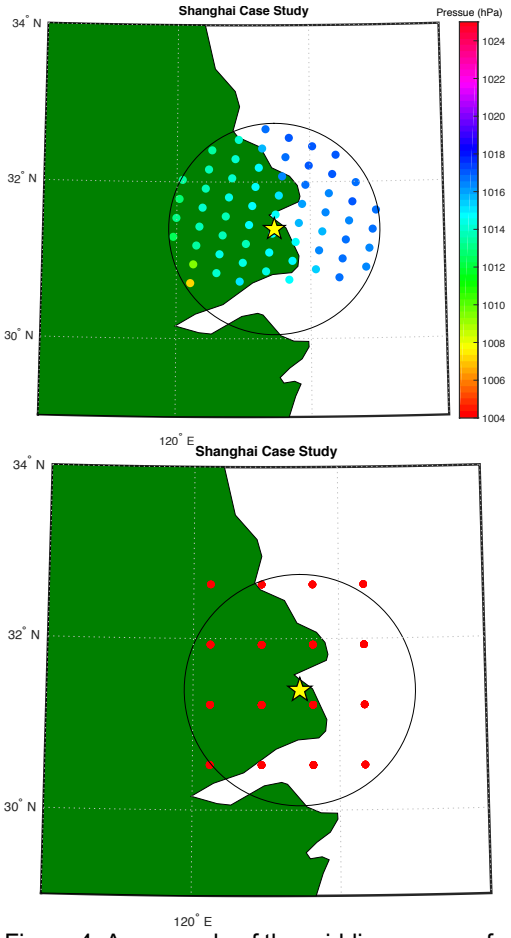

Figure 4. An example of the gridding process for Shanghai. The upper is the original data from GIIRS and the bottom image is the GIIRS data gridded to the ERA-I latitude and longitude. The yellow star represents the radiosonde launch location.

2.4 Statistical Analysis

To obtain statistical indicators like RMSE, standard deviation and percent yield, profiles within 150 km were used for comparison to MADIS radiosondes. Each of 101 levels was compared separately. The MADIS radiosondes were interpolated to the same 101 levels for best comparison. Figure 5 shows an example sounding for Shanghai for the radiosonde and GIIRS temperature and dewpoints. For the day June 1, 2018, the temperature RMS differences range from 0 to 3 K, and the dewpoint RMS differences range from 5 to 10 K, as shown in example Figure 6. The variability at these two case study locations for all of the case study days analyzed is summarized in Table 3 as maximum RMS errors.

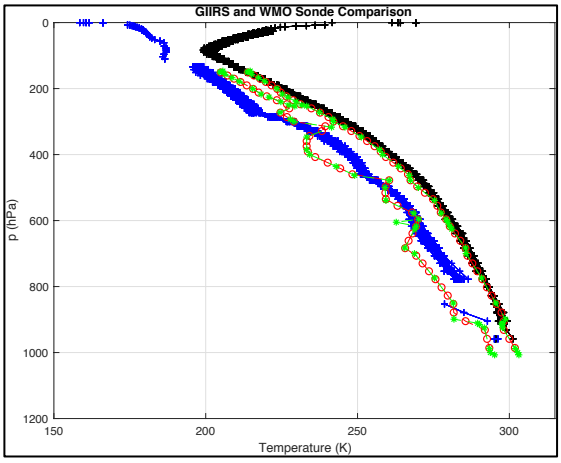

Figure 5. Shows the local sounding in green with the interpolated sounding over-layed in red. The black lines represent all of the GIIRS temperature profiles within the domain and the blue represent the dewpoint profiles.

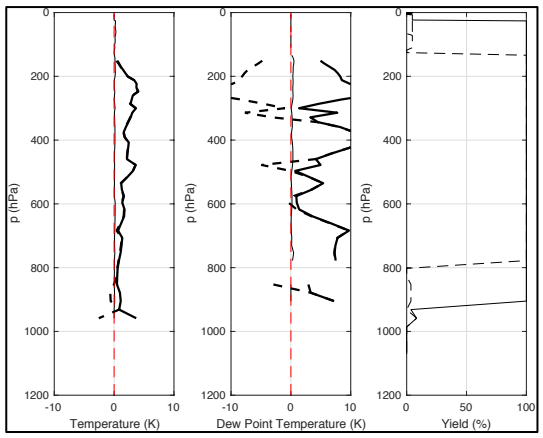

Figure 6. The RMSE (bold solid), difference (dashed) and standard deviation (solid) for both temperature (left) and dew point (middle). The total yield at each vertical level is the right most panel.

2.5 Quality Control

The quality control process in this study was varied between data sets. GIIRS data was selected using the given quality control product. The CMA has four quality control levels with the following meanings 0=perfect, 1=good, 2=bad, 3=do not use. Quality control level 2 was used in this study. Quality control was already applied for MADIS surface stations and is included in the final product. MADIS radiosonde stations included quality control.

3. Conclusions

Despite the limited statistical dataset a number of conclusions can be drawn from this preliminary study. First, validation sites were identified within the GIIRS domain with upper air soundings from radiosonde launch sites and surface observation from surface met stations. Case studies for two locations were evaluated: Shanghai, China and Darwin, Australia. Validation data from the WMO radiosonde network and NOAA MADIS were used at these locations. In addition, GIIRS preliminary soundings from the Chinese Meteorological Agency (CMA) were downloaded from http://www.cma.gov.cn

Representative cases were selected for mostly clear sky conditions to illustrate the comparison methodology of GIIRS retrieved profiles with a nearby WMO radiosonde. Preliminary statistics suggest temperature bias is less than 3 K with standard deviation much less than 1 K. Dewpoint temperature bias is 5-10 K with standard deviation less than 1 K.

In future studies, special attention will be made to validation of the diurnal dependence of surface observations of air temperature and dewpoint for assessment of atmospheric stability; CAPE, CIN, Lifted Index, etc. Figure 7 illustrates an example diurnal cycle for Shanghai on March 2, 2018. It is clear that temperature increases between 0 and 10 UTC. This is typical of solar heating of the surface considering sunset in shanghai is at 10 UTC. In addition, the MADIS observations show a decrease in dewpoint between 4 and 14 UTC, possibly due to the land sea breeze effect. In this case, GIIRS surface temperature and dewpoint estimates are too high. GIIRS data will be used to assess the diurnal sampling of the boundary layer from the unique geostationary of the FY4A platform.

This study is in support of a larger project to develop validation methods for the evaluation of Geo and Leo sounders to assess the ability of satellite passive sounders to monitor the diurnal characteristics of the planetary boundary layer. The EUMETSAT METEOSAT Third Generation (MTG) IRS sounder will provide geostationary information similar to GIIRS starting in about 2023.

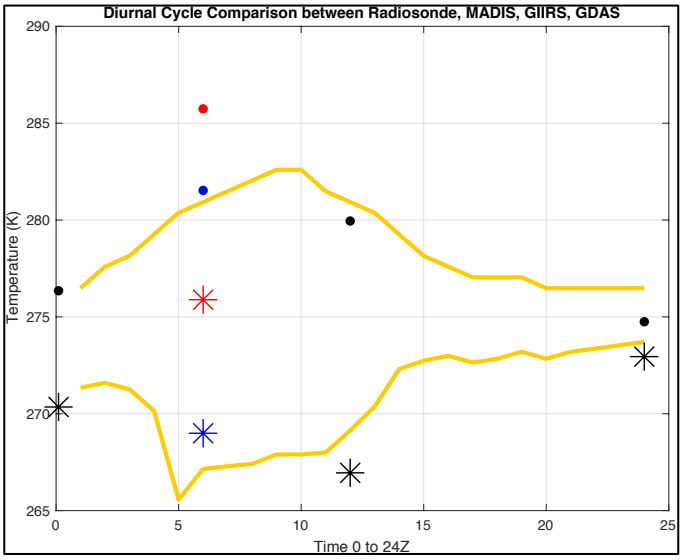

Figure 7. Diurnal Temperature and dewpoint cycle for shanghai on Mary 2, 2018. The blue colored dots and stars are GDAS model data, the red dots and stars and GIIRS satellite data, the black colored dots and stars are local station radiosonde data and the yellow lines represent the continuous MADIS sampling of temperature (top) and dewpoint (bottom). The dots are samples of temperature and the stars are dewpoint measurements.

4. References

Bian, J., Chen, H., Vomel, H., Duan, Y., Xuan, Y., & Lu, D. (2011). Intercomparison of Humidity and Temperature Sensors: GTS1, Vaisala RS80, and CFH. *Advances in Atmospheric Sciences*, *28*(1), 139–146. https://doi.org/10.1007/s00376-010-9170-8.1.Introduction

Feng, L. (2006). New Development with Upper Air Sounding in China. *WMO*, *94*(1354).

Kottayil, A., Buehler, S. A., John, V. O., Miloshevich, L. M., Milz, M., & Holl, G. (2012). On the importance of Vaisala RS92 radiosonde humidity corrections for a better agreement between measured and modeled satellite radiances. *Journal of Atmospheric and Oceanic Technology*, *29*(2), 248–259. https://doi.org/10.1175/JTECH-D-11-00080.1

Vömel, H., David, D. E., & Smith, K. (2007). Accuracy of tropospheric and stratospheric water vapor measurements by the cryogenic frost point hygrometer: Instrumental details and observations. *Journal of Geophysical Research Atmospheres*, *112*(8), 1–14. https://doi.org/10.1029/2006JD007224

Vomel, H., Selkirk, H., Miloshevich, L., Valverde-Canossa, J., Valdes, J., Kyro, E., … Diaz, J. A. (2007). Radiation Dry Bias of the Vaisala RS92 Humidity Sensor. *Australasian Journal of Educational Technology*, *24*, 953–963. https://doi.org/10.1175/JTECH2019.1

Yang, J., Zhang, Z., Wei, C., Lu, F., & Guo, Q. (2017). Introducing the new generation of Chinese geostation ary weat her satellites, Fengyun-4. *Bulletin of the American Meteorological Society*, *98*(8), 1637–1658. https://doi.org/10.1175/BAMS-D-16-0065.1

5. Tables

Table 1. Summary of the characteristics of the GTS1 Radiosonde.

GTS1 Digital Radiosonde Technical Parameters	
Temperature White Rod Thermistor	
Range	+50°C~ -90°C
Accuracy (standard deviation)	+50°C~ -80°C 0.2°C -80°C~ -90°C 0.3°C
Resolution	0.1°C
Humidity Carbon Film Lamellar Hygristor	
Range	0%RH ~ 100%RH
Accuracy (standard deviation)	15%RH ~ 95%RH T≥-25°C 5%RH T< -25°C 10%RH
Resolution	1%RH
Pressure Silicon electric-bridge pressure sensor	
Range	1060hPa ~ 5hPa
Accuracy (standard deviation)	1050hPa ~ 500hPa 2hPa 500hPa ~ 5hPa 1hPa
Resolution	0.1hPa
Measurement cycle for PTU sensors	1.2sec

Table 2. Summary of the characteristics of the Vaisala RS92 radiosonde.

Vaisala RS92 Technical Parameters	
Temperature Capacitive Wire	
Range	+60°C~ -90°C
Accuracy (standard deviation)	1080-100 hPa 0.2°C 100-20 0.3 hPa 0.3°C 20-3 hPa 0.5°C
Resolution	0.1°C
Humidity Thin-Film Capacitor Heated Twin Sensor	
Range	0 %RH ~ 100 %RH
Accuracy (standard deviation)	2 %RH
Resolution	1%RH
Pressure Silicon	
Range	1080hPa ~ 3hPa
Accuracy (standard deviation)	1080hPa ~ 100hPa 0.5hPa 100hPa ~ 3hPa 0.3hPa
Resolution	0.1hPa
Measurement cycle for PTU sensors	1 sec

Table 3. Summary of the RMSE temperature and dewpoint maximum error for the case study days and locations.

Location	Shanghai		Darwin	
Clear Days	RMSE Temperature Range	RMSE Dewpoint Range	RMSE Temperature Range	RMSE Dewpoint Range
June 1	<4K	<15K	<7K	<15K
June 11	-	-	<3K	3-10K
July 14	<3K	<10K	<3K	<10K
July 15	<3K	<10K	<5K	<10K
July 25	-	-	<4K	<10K

6. Author's Corresponding Address

Jessica Gartzke
jmgartzke@wisc.edu
1225 West Dayton Street Madison WI, 53706

7. Acknowledgements

This work was supported by NOAA Cooperative Agreement NA15NES4320001.